Japanese Journal of Ophthalmology (2019) 63:82–89
https://doi.org/10.1007/s10384-018-0631-4

THE OFFICIAL INTERNATIONAL JOURNAL OF THE JAPANESE OPHTHALMOLOGICAL SOCIETY

CLINICAL INVESTIGATION

Kago-Eye2 software for semi-automated segmentation of subfoveal choroid of optical coherence tomographic images

Shozo Sonoda[1] · Hiroto Terasaki[1] · Naoko Kakiuchi[1] · Hideki Shiihara[1] · Tomonori Sakoguchi[1] · Masatoshi Tomita[1] · Yuki Shinohara[1] · Takehiro Yamashita[1] · Eisuke Uchino[1] · Taiji Sakamoto[1]

Received: 9 January 2018 / Accepted: 30 August 2018 / Published online: 24 October 2018

Abstract

Purpose To determine the capabilities of the "Kago-Eye2" software to semi-automatically segment the choroid in the optical coherence tomographic (OCT) images.

Study design A cross-sectional, prospective study of 44 healthy volunteers.

Methods The Kago-eye2 software was developed to detect the border between Choriocapillaris and Sattler's layer (C–S) and between Sattler's layer and Haller's layer (S–H). The intra- and inter-grader agreements were determined for the segmentations made with semi-automated and manual analysis using the Kago-Eye2 software. The inter-method agreements were determined for two independent graders.

Results Forty-four right eyes of 44 heathy volunteers (22 men) with a mean age of 35.0 ± 8.8 years were studied. The intra-grader agreement of the C–S border was 0.97 for grader 1 and 0.892 for grader 2 for the manual segmentation, and 0.908 for grader 1 and 0.842 for grader 2 for the Kago-Eye2 segmentation. For the S–H border, the intra-grader agreement was 0.96 for grader 1 and 0.981 for grader 2 for manual segmentation and 0.855 for grader 1 and 0.839 for grader 2 with the Kago-Eye2. For the C–S and S–H border, the inter-grader agreement was 0.548 and 0.902 for manual segmentation and 0.947 and 0.833 for the Kago-Eye2. The inter-method agreement was 0.565 for the C–S border and 0.759 for the S–H border.

Conclusion The Kago-Eye2 software can segment the layers of the subfoveal choroid with good reproducibility and repeatability. We conclude that the Kago-Eye2 software can be used for semi-automatic segmentation of the choroidal layers.

Keywords EDI-OCT · Choroid · Image binarization · Kago-Eye2

Introduction

Evidence has been accumulating that the choroid plays important roles in different types of retinal diseases [1–9]. The evidence has been collected since the introduction of enhanced depth imaging optical coherence tomography (EDI-OCT) [2]. Thus, the choroid of normal eyes and eyes with different types of retinal diseases has become an important structure for investigations by clinicians and researchers [10].

Initial studies of the choroid in the OCT images were mostly measurements of its thickness [3, 11–13] and a different evaluation method was needed to examine the choroidal structure in more detail [14–16]. The choroid is a network of vessels and stromal tissue, and it consists of three layers; the choriocapillaris (CC) immediately beneath the retinal pigment epithelial (RPE) layer with a thickness of approximately 10 μm, Sattler's layer, composed of small and middle diameter blood vessels, and Haller's layer composed of large diameter vessels [1]. It has been reported that the inner and outer layers of the choroid were affected differently by different types of retinochoroidal diseases [17, 18]. Thus, it is necessary to investigate the changes of each layer to understand the effects of choroidal alterations on the development and progression of retinochoroidal diseases.

Corresponding author: Taiji Sakamoto

Electronic supplementary material The online version of this article (https://doi.org/10.1007/s10384-018-0631-4) contains supplementary material, which is available to authorized users.

✉ Taiji Sakamoto
tsakamot@m3.kufm.kagoshima-u.ac.jp

[1] Department of Ophthalmology, Kagoshima University Graduate School of Medical and Dental Sciences, Kagoshima, Japan

Unlike histological examinations of the choroid, it is not easy to distinguish the borders of the three layers of the choroid in the OCT images. Currently, the boundaries of each layer are selected manually, but it is easy to be biased and the reproducibility is not high. To create a reliable and accurate method, a technique for automated choroidal stratification is needed.

We recently developed a software, named the "Kago-Eye2", that semi-automatically performs the segmentation between the choriocapillaries and Satller's layer and between Sattler's layer and Haller's layer. As best we know, there is no other software that stratifies the layers of the choroid in the OCT images automatically.

Thus, the purpose of this manuscript is to present the characteristics of the Kago-Eye2 software, and to explain how it is used in normal eyes. We also compared the findings with that of manual segmentation.

Methods

Subjects

This was a cross sectional, prospective study of 44 eyes of 44 volunteers that was conducted with the approval of the Ethics Committee of Kagoshima University Hospital, Kagoshima, Japan. It was registered with the University Hospital Medical Network (UMIN)-clinical trials registry (CTR) in November 2013. The registration title is "UMIN000012310, Choroidal structure on OCT images for healthy eyes". A detailed protocol is available at, http://www.kufm.kagoshima-u.ac.jp/~op/gairai/RCstructurestudy.html. A written informed consent was obtained from all the subjects after an explanation of the procedures to be used and possible complications. All of the procedures conformed to the tenets of the Declaration of Helsinki.

Prior to the measurements, all of the eyes had a comprehensive ocular examination which included slit-lamp examinations of the anterior segment of the eye and ophthalmoscopy of the fundus. The intraocular pressure was measured with a pneumotonometer (CT-80, Topcon, Tokyo, Japan), and the axial length was measured with the AL-2000 ultrasound instrument (Tomey, Tokyo, Japan). The best-corrected visual acuity (BCVA) was measured after determining the refractive error with an Auto Kerato-Refractometer (RM8900, Topcon). If both eyes met the inclusion and exclusion criteria, only the right eye was analyzed.

The eligibility criteria were age ≥18-years and the eye normal as determined by ophthalmoscopy and OCT. The exclusion criteria were eyes with known ocular diseases such as glaucoma and diabetic retinopathy, presence of systemic diseases such as hypertension and diabetes, high myopia of more than -6.0 D, prior intraocular surgery or injections, and eyes in which the ocular fundus could not be observed due to media opacities. None of the eyes was excluded due to poor quality OCT images because of poor fixation.

Choroidal images obtained by spectral-domain optical coherence tomography (SD-OCT)

Cross-sectional choroidal images were obtained by EDI-OCT as described in detail [14, 15]. The scans were 7 horizontal lines of 30 x 10 degrees through the center of the fovea made with a Heidelberg Spectralis OCT instrument (Spectralis; Heidelberg Engineering, Heidelberg, Germany). Each image was obtained using the eye tracking system, and 100 scans were averaged. All of the eyes were examined without mydriasis.

Because there are significant diurnal fluctuations of the choroidal thickness, all of the examinations on a single subject were done within one hour on the same day between 11:00 to 13:00 hours. The images centered on the fovea were used for the analyses.

Image processing by segmentation algorithm of Kago-Eye2

The Kago-Eye2 software was written in C++ programing language and was written to detect the borders between choroiocapillaris and Sattler's layer (C-S border) and that between Sattler's layer and Haller's layer (S-H border) in the OCT images. A detailed protocol is available in our previous paper on the processes between steps 1 and 3 [16].

1. Preprocessing

1-1. The software obtains the image data as tiff or bmp images from the OCT device. White on black images are recommended, and Tiff images were used in this study.

1-2. The scale of each image was adjusted by filling out the form on the screen. The scales for the X-axis and Y-axis are specified for each OCT model. In the Heidelberg Spectralis OCT instrument, this information is available in the embedded software (Supplemental File S2).

1-3. A square-shaped region of interest (ROI) was determined on the screen. It is recommended that the entire width of the retina in the image is selected as ROI.

1-4. Align the left and right borders of the ROI so that the fovea is at the center.

1-5. Rotate the image so that the retinal pigment epithelium (RPE) is oriented horizontally. If necessary, steps 1-4 and 1-5 can be skipped because these steps do not affect the results.

1-6. Three representative vascular lumens in Haller's layer of the OCT image that were the darkest were selected manually by clicking on their center. The averaged reflectivity of these three lumens, expressed as brightness tone, was used as a reference of the lowest cut-off value of the brightnesses. Using these data, the clipped image was transformed to a new image with 256 tones [0 to 255].

2. Determination of threshold

2-1. A histogram was constructed by the brightness of each pixel in the ROI of the image.
2-2. Obtain the threshold value. Create a distribution of the brightnesses (Fig. 1a, middle). Our previous study showed that the threshold value should be set to 4 or 5, which means that the top 4 or 5% of the brightest pixels turn white after banalization because the RPE layer is the brightest layer [19].
2-3. Binarize the image using the binarization threshold obtained in step 2 (Fig. 1a, right).

3. Creation of RPE layer boundary and chorioscleral boundary

3-1. The boundaries of the black and white areas (lower margins of the RPE) are detected in the binarized image by the contour extraction method. The software is programmed to mark the lower boundary of the white band with a light blue-colored line. This line indicates the boundary between RPE and choroid and is used for the following analyses.
3-2. The chorioscleral boundary is selected manually.

4. Creation of choriocapillaris border

4-1. Extract the brightness data for 50 pixels (Fig. 1b, yellow arrows) along the vertical direction beginning from the RPE line to bottom (Fig. 1b, red pixels).
4-2. Place them in a rectangle to make all heights uniform (Fig. 1b, right).
4-3. Average the brightness of the pixels in the same horizontal line (Fig. 1b, right).
4-4. The results of averaging is analyzed by the second derivatives from top to the bottom.
4-5. When the number in the pixel calculated by second derivative is 0 and is continued twice in a row or less than 0, the corresponding pixel is set as the boundary of the choriocapillaris. As a result, the distance from the RPE layer to the pixel is set to be the thickness of the choriocapillaris.

5. Creating the border between Sattler's layer and Haller's layer

5-1. Extract the brightness data of each pixel vertically from the RPE layer to the choroid-scleral boundary (Fig. 1c, left, pink arrows).
5-2. The change in the brightness of the pixels of single column from top to bottom is determined by the second derivatives (c, right). First, the pixels at which the value changes from plus to minus are chosen by the second derivatives (candidates). Then the border was determined to be the pixel with the highest number by the first derivatives among the candidates. The first border from RPE layer is the one between choriocapillaris (CC) and Sattler's layer. The second border is taken to be the border between Sattler's layer and Haller's layer. This processing is done for every column.
5-3. The pixels chosen in previous steps of each column is placed as pixel with a red margin (Fig. 1d). Then the data are fitted by a quadratic equation using the least squares method (Fig. 1d, red intermittent line). Although this software is able to perform curve fitting by quadratic to 6th curve, the default setting is done by quadratic curve. This line is taken to be the border between Sattler's layer and Haller's layer.

Regional differences of choriocapillaris thickness

The Kago-Eye2 software determined the distance from the RPE layer to the border between choriocapillaris and Sattler's layer, the choriocapillaris thickness, as a line tangent to the RPE layer. Thus, we examined whether the choriocapillaris thickness differed in different regions of the eyes of healthy subjects. The thickness of the choriocapillaris in different regions such as subfovea, 750 and 1500 µm nasal and temporal from fovea were manually measured in the SD-OCT images with the embedded caliper in a Heidelberg Spectralis OCT instrument.

Agreement between results obtained semi-automated and manual analysis with the Kago-Eye2 software

The results obtained semi-automatically and manually with the software to segment the choroid were compared. Horizontal choroidal images through the fovea were obtained with the Spectralis OCT device as described [20]. The borders of the CC-Sattler's layer and Sattler's layer-Haller's layer were determined semi-automatically with the Kago-Eye2 software as indicated above. The distance of the indicated pixel from RPE layer could be manually measured by the Kago-Eye2 software. Thus, manual measurement was

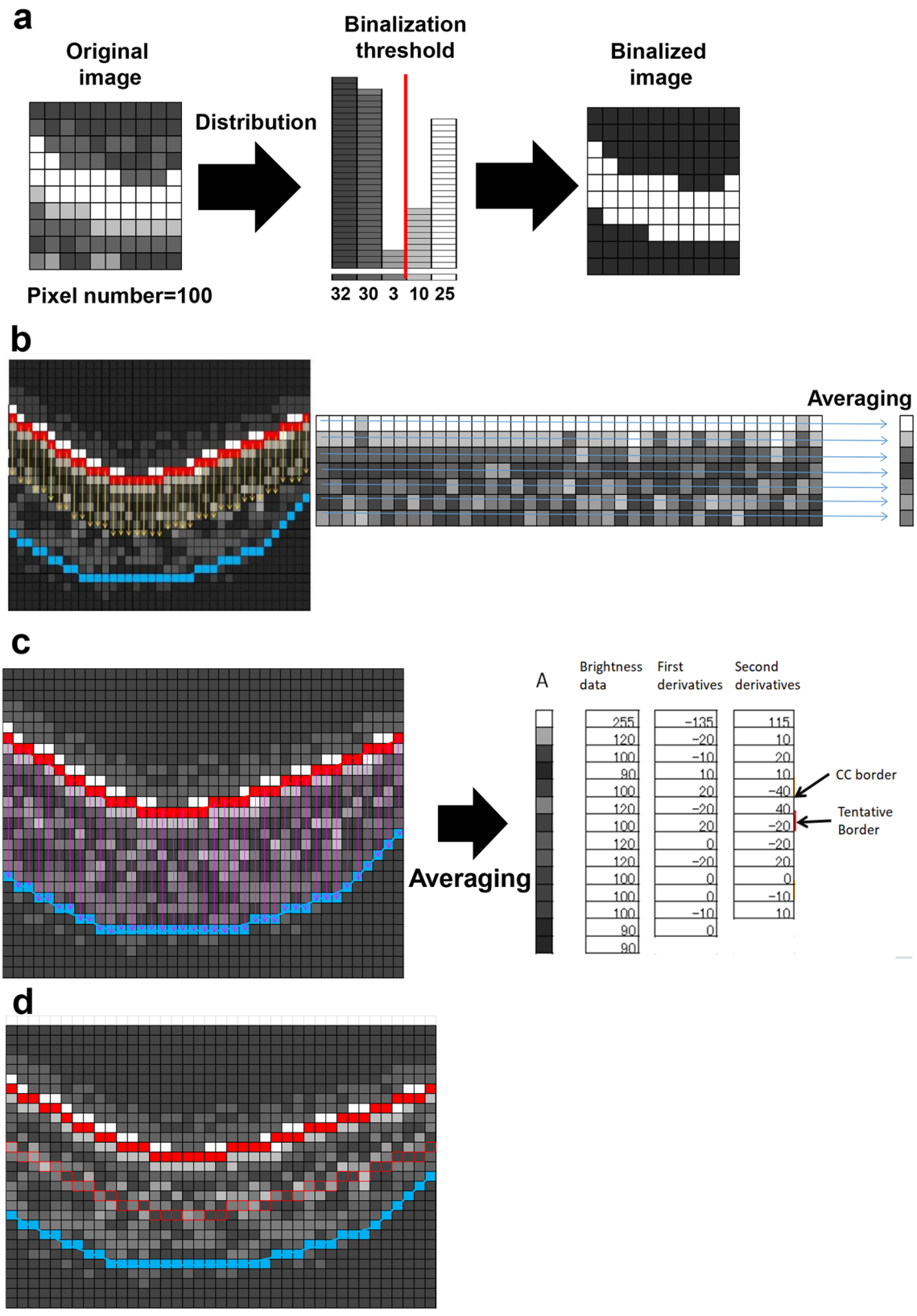
a
Original image
Distribution
Binalization threshold
Binalized image
Pixel number=100
32 30 3 10 25
b
Averaging
c
A
Brightness data
First derivatives
Second derivatives
255 120 100 90 100 120 100 120 120 100 100 100 90 90
−135 −20 −10 10 20 −20 20 0 −20 0 0 −10 0
115 10 20 10 −40 40 −20 −20 20 0 −10 10
CC border
Tentative Border
Averaging
d

◂**Fig. 1** **a** Creating a brightness distribution. The distribution of the brightnesses is created to obtain the threshold value (middle). It is recommended that threshold value is set to 4 or 5, which means the top 4 or 5% of the brightest pixels turns white after banalization. The image is then binarized with the threshold (right). **b** Conceptional image of the RPE and choriocapillaris represented by different shades of gray pixels. The RPE layer is represented by the red pixels and the chorioscleral border by the blue pixels. The brightness of each of the 50 pixels below the RPE layer (yellow arrows) is extracted vertically and the brightness of each line is averaged horizontally. **c** Conceptional image of brightness data of choroid for each pixel. In this image, the RPE layer is represented by the red pixels, and the chorioscleral boundary by the blue pixels. The choroidal thickness at each point is expressed by the length of the pink arrows. The brightness of each pixel is expressed as a shade between white and black; white represents high brightness, and black represents low brightness. A pixel expressing the CC border is indicated by an arrow. A tentative border pixel is indicated by another arrow (right). *CC* choriocapillaris. **d** Conceptional image of brightness data of choroid. In this image, the RPE layer is represented as red pixels and chorioscleral boundary is blue. The pixels suggesting the border between Sattler's and Haller's layer were determined by the combination of the first and second derivatives. Then a fitting curve was determined using the least squares method. The red intermittent line represents the border between Sattler's layer and Haller's layer

performed with this method. The same images were analyzed by the two experienced examiners on different days to avoid measurement bias. The order of the manual and automatic measurements was performed randomly.

Next, the inter-rater agreement with the software was calculated. This analysis was done by two independent graders (HT and SS) to determine the inter-rater agreement. The intra-rater and inter-method agreements were determined for the two graders.

Statistical analyses

All statistical analyses were performed with the SPSS statistics 19 for Windows (SPSS Inc., IBM, Somers, NY). The inter-rater correlation coefficients were calculated by a two-way mixed-effects model for measurements of absolute agreement. Bland-Altman plots were created to assess the agreement of measurements between the semi-automated and manual measurements with the Kago-Eye2 software. A P value of <0.05 was taken to be statistically significant.

Results

Forty-four right eyes of 44 heathy volunteers (22 men and 22 women) were studied. The average age of the volunteers was 35.0 ± 8.8 years (average ± SD) with a range of 28 to 56 years. The mean BCVA was -0.10 ± 0.06 logMAR units, and the mean refractive error (spherical equivalent) was -2.88 ± 1.96 diopters (D). The mean axial length was 24.86 ± 1.02 mm, and the mean intraocular pressure (IOP) was 14.4 ± 3.2 mmHg. Although the mean refractive error was slightly myopic, clear OCT images of the choroid were obtained from all eyes.

Regional differences of choriocapillaris thickness

The thickness of the choriocapillaris was 18.1 ± 2.93 μm at the fovea, 18.3 ± 2.81 μm at 750 μm and 17.2 ± 3.69 μm at 1500 μm temporal from the fovea and 17.6 ± 2.55 μm at 750 μm and 17.8 ± 2.57 μm at 1500 μm nasal from the fovea. The differences in the thicknesses among the regions were not significant (Supplemental Table S1).

Intra-rater agreements

The segmentation of the choroid was done manually by two graders independently or semi-automatically with the Kago-Eye2 software. The results showed that the intraclass correlation coefficients (ICCs) of intra-rater agreement for CC-Sattler's border by the manual segmentation was 0.97 for Grader 1 and 0.892 for Grader 2 (Table 1). The ICC for the S-H border was 0.96 for Grader 1 and 0.981 for Grader 2 (Table 1). The ICCs of the intra-rater agreement of the C-S border by the semi-automated segmentation was 0.908 for Grader 1 and 0.842 for Grader 2 (Table 2). For the S-H border by semi-automated segmentation, the ICCs was 0.855 for Grader 1 and 0.839 for Grader 2 (Table 2).

Inter-rater and inter-methods agreements

The inter-rater agreement between the results obtained manual and with the semi-automated segmentation performed by the 2 graders were examined (representative case was shown in Fig. 2). The results showed that the inter-rater agreement of the C-S border and the S-H border by the manual method were 0.548 and 0.902, respectively (Table 3). The inter-rater agreements of the C-S border and the S-H border determined by the semi-automated method were 0.947 and 0.833 (Table 3). The inter-method coefficients, i.e., manual vs semi-automated measurements, of the C-S and S-H border were 0.565 and 0.759 by Grader 1 and 0.543 and 0.763 by Grader 2 (Table 4).

Bland-Altman analyses

There was no fixed bias or proportional bias between the results obtained with the automated and manual methods (Fig. 3).

Discussion

The results showed that the Kago-Eye2 software can detect the borders between the CC and Sattler's layer and that between Sattler's layer and Haller's layer in the OCT images

Table 1 Intra-rater agreement for manual segmentation

	CC-Sattler border	95% CI	Sattler-Haller border	95% CI
Grader 1	0.97	0.946 - 0.983	0.96	0.928 - 0.978
Grader 2	0.892	0.811 - 0.939	0.981	0.965 - 0.989

CC choriocapillaris, *CI* confidence interval

Table 2 Intra-rater agreement of semi-automated segmentation

	CC-Sattler border	95% CI	Sattler-Haller border	95% CI
Grader 1	0.908	0.839 - 0.91	0.855	0.75 - 0.918
Grader 2	0.842	0.729 - 0.91	0.839	0.724 - 0.909

CC choriocapillaris, *CI* confidence interval

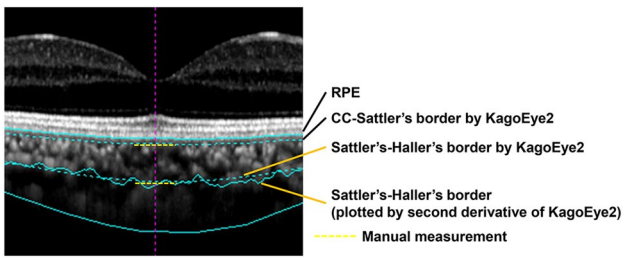

Fig. 2 Representative image of the choroid segmented manually or by the Kago-Eye2 software. Solid line and dotted line in Sattler's-Haller's border represents the border determined by second derivative (see Methods) and by the least squares method by KagoEye-2, respectively. Choriocappilaris-Sattler's layer and Sattler's layer-Haller's layer borders are clearly segmented. Dotted red line represents the results by manual measurement which is a good fit with the values obtained by the automated method

with high inter-rater and intra-rater coefficients of correlation (Fig. 2). To the best of our knowledge, a software has not been published which can segment these layers in the OCT images semi-automatically.

The CC is the layer of blood vessels between the RPE and Sattler's layer. Histological analyses have shown that the thickness of the CC is between 5 to 10 µm [21]. However, because the CC does not have vascular tone to maintain its form after enucleation, there is a high possibility that the histological thickness differs from that in the living tissue. Although OCT has enabled clinicians and researchers to measure the thickness of the choriocapillaris in the living tissues reliably, there is no final agreement on the thickness, e.g., some reported it to be 10 µm and others 50 µm or even thicker [22, 23].

Preliminary experiments have shown that there were almost no regional differences in the distance between the CC and the RPE layer (Supplemental Table S1). Thus, a line tangent to the RPE was taken to be the boundary between CC and Sattler's layer, and it was set to have a value of 0 by secondary differentiation of each depth. This means that the degree of change of the brightness came to a plateau at this point.

The thickness of the CC measured manually was 16.10 ± 2.74 µm for Grader 1 and 17.29 ± 2.50 µm for Grader 2. On the other hand, the automated measurements with the with Kago-Eye2 indicated that the thickness was 17.24 ± 3.06 µm by Grader 1 and 17.33 ± 3.18 µm by Grader 2. The intra-rater agreement was 0.97 for Grader 1 and 0.892 for Grader 2 by manual measurements, and it was 0.908 for Grader 1 and 0.842 for Grader 2 by the Kago-Eye2 software. Thus, the reproducibility was good and approximately the same for both manual and automated measurements. On the other hand, the inter-rater agreement was 0.947 for the automated measurements compared to 0.548 with the manual

Table 3 Inter-rater agreement by semi-automated and manual measurements

	Grader 1 (µm ± SD)	Grader 2 (µm ± SD)	ICC	95% CI
CC-Sattler border (manual)	16.10 ± 2.74	17.29 ± 2.50	0.548	0.264 - 0.736
CC-Sattler border (auto)	17.24 ± 3.06	17.33 ± 3.18	0.947	0.906 - 0.971
Sattler-Haller border (manual)	104.47 ± 29.96	101.83 ± 27.41	0.902	0.828 - 0.945
Sattler-Haller border (auto)	104.37 ± 23.19	104.05 ± 26.70	0.833	0.714 - 0.906

CC choriocapillaris, *CI* confidence interval, *SD* standard deviation

Table 4 Inter-method agreement of semi-automated and manual measurements by 2 graders

	manual (µm ± SD)	Automated (µm ± SD)	ICC	95% CI
CC-Sattler border (Grader 1)	16.10 ± 2.74	17.24 ± 3.06	0.565	0.30 - 0.7425
Sattler-Haller border (Grader 1)	101.83 ± 27.41	104.05 ± 26.70	0.759	0.598 - 0.861
CC-Sattler border (Grader 2)	17.29 ± 2.50	17.33 ± 3.18	0.543	0.294 - 0.722
Sattler-Haller border (Grader 2)	104.47 ± 29.96	104.37 ± 23.19	0.763	0.606 - 0.863

CC choriocapillaris, *CI* confidence interval, *SD* standard deviation

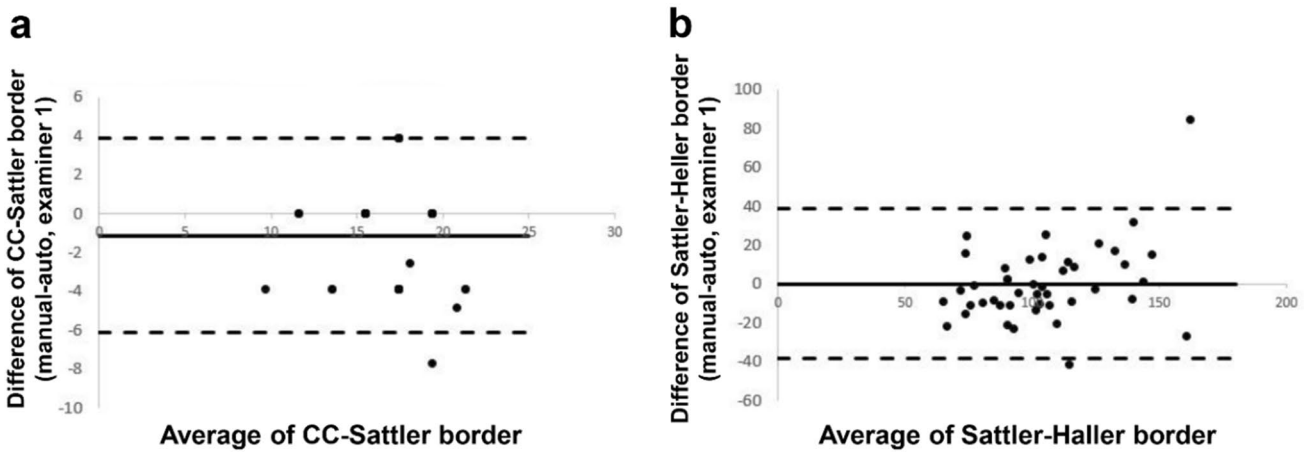

Fig. 3 Bland-Altman analysis of manual and automated analyses of the segmentation of the subfoveal choroid. The results for the border between choriocapillaris and Sattler's layer (**a**) and that between Sattler's layer and Haller's layer (**b**) are shown. There was no systemic error between manual and automatic measurements

measurements indicating the superiority of the automated measurements.

The ICC of the inter-method agreements for the CC-Sattler's border was 0.565 for Grader 1 and 0.543 for Grader 2. Actually, the difference between the absolute values by the manual measurements and automated measurements was very small; a 1.14 μm for Grader 1 and 0.04 μm for Grader 2. With the current OCT device, even if it is shifted by 1 pixel in the vertical direction, the value of the distance would change by 3.5 μm [24, 25]. The Bland-Altman analysis showed the difference between manual and automated measurement was within 1 μm. Therefore, it is possible that the Kago-Eye2 software can be a practical and useful method to segment the choroid.

In the segmentation of Sattler's and Haller's layers, we took a different approach from that between the CC and Sattler's layer because the border between Sattler's and Haller's layer is not necessarily parallel to Bruch's membrane. Therefore, the brightness of each pixel in the vertical direction was secondarily differentiated in the same way as it was for the border between CC and Sattler's layer, and the pixel where the brightness changed from bright to dark determined by a second derivative was chosen as the S-H border point. The point was plotted for each pixel in the different columns, and a best-fit line was drawn through these points by the least squares method to determine the boundary between Sattler's layer and Haller's layer. As a result, Grader 1 measured the border at 104.47 ± 29.96 μm and Grader 2 at 101.83 ± 27.41 μm for the manual measurements. The intra-rater agreement by manual method was 0.96 in Grader 1 and 0.981 in Grader 2 which was sufficiently high. In the automated selections, Grader 1 measured the point at 104.37 ± 23.19 μm and Grader 2 at 104.05 ± 26.7 μm. The intra-rater agreement by semi-automated method was 0.855 for Grader 1 and 0.839 for Grader 2 which was sufficiently high. In addition, the inter-method agreement was 0.759 for Grader 1 and 0.763 for Grader 2. Thus, the reproducibility between the two methods was very good.

There are many advantages of the semi-automated analyses of the OCT images. With the manual procedures, the ability, proficiency, and experience of the examiner inevitably affect the results. Because our graders were experienced and skilled in image analyses, there was high agreement even in the manual measurements. However, in cases of a non-experienced grader, a highly accurate measurement would probably not be achieved. In addition, the advantage of the semi-automated measurements is evident when comparing different studies or analyzing data measured by different individuals in a large-scale research. Furthermore, it is difficult to follow the changes in the brightness of every pixel manually which would require considerable amount of time. Therefore, this method which can semi-automatically stratify the OCT choroidal image would be very practical and important.

In conclusion, our new software algorithm can select the borders of the different layers of the subfoveal choroid in normal eyes automatically, and the findings were consistent with the manual analysis. The results cannot be applied to areas other than the macular area and the study in the disease eye is the next task. The present software was able to accurately identify the boundary of CC, Sattler's layer, and Haller's layer. The position of each border under the macula in the normal eyes was highly repeatable between the graders. Considering the advantages of the semi-automated stratification of choroid of the OCT images, this software should have many uses.

Acknowledgements The authors thank Professor Emeritus Duco Hamasaki of the Bascom Palmer Eye Institute of the University of Miami for providing critical discussions and suggestions to our study and revision of the final manuscript. This study was supported by JSPS KAKENHI Grant number 15H04996.

Funding The funding organizations had no role in the design or conduct of this research.

Conflicts of interest None of the authors has any conflict of interest in any materials, software or methods in this manuscript.

References

1. Castro-Correia J. Understanding the choroid. Int Ophthalmol. 1995;19:135–47.
2. Imamura Y, Fujiwara T, Margolis R, Spaide RF. Enhanced depth imaging optical coherence tomography of the choroid in central serous chorioretinopathy. Retina. 2009;29:1469–73.
3. Laude A, Cackett PD, Vithana EN, Yeo IY, Wong D, Koh AH, et al. Polypoidal choroidal vasculopathy and neovascular age-related macular degeneration: same or different disease? Prog Retin Eye Res. 2010;29:19–29.
4. Lutty GA, Cao J, McLeod DS. Relationship of polymorphonuclear leukocytes to capillary dropout in the human diabetic choroid. Am J Pathol. 1997;151:707–14.
5. Saito M, Kano M, Itagaki K, Ise S, Imaizumi K, Sekiryu T. Subfoveal choroidal thickness in polypoidal choroidal vasculopathy after switching to intravitreal aflibercept injection. Jpn J Ophthalmol. 2016;60:35–41.
6. Yoshikawa M, Akagi T, Nakanishi H, Ikeda HO, Morooka S, Yamada H, et al. Longitudinal change in choroidal thickness after trabeculectomy in primary open-angle glaucoma patients. Jpn J Ophthalmol. 2017;61:105–12.
7. Pablo LE, Bambo MP, Cameo B, Ferrández B, Güerri N, Polo V, et al. The use of zonal analysis of peripapillary choroidal thickness in primary open-angle glaucoma. Jpn J Ophthalmol. 2018;62(1):41–7.
8. Song YJ, Kim YK, Jeoung JW, Park KH. Assessment of peripapillary choroidal thickness in primary open-angle glaucoma patients with choroidal vascular prominence. Jpn J Ophthalmol. 2017;61:448–56.
9. Enaida H, Nagata S, Takeda A, Nakao S, Ikeda Y, Ishibashi T. Changes in chorioretinal blood flow velocity and cerebral blood flow after carotid endarterectomy. Jpn J Ophthalmol. 2016;60:459–65.
10. Spaide RF, Koizumi H, Pozzoni MC. Enhanced depth imaging spectral-domain optical coherence tomography. Am J Ophthalmol. 2008;146:496–500.
11. Kim JH, Kang SW, Kim JR, Kim SJ. Variability of subfoveal choroidal thickness measurements in patients with age-related macular degeneration and central serous chorioretinopathy. Eye (Lond). 2013;27:809–15.
12. Rayess N, Rahimy E, Ying GS, Bagheri N, Ho AC, Regillo CD, et al. Baseline choroidal thickness as a predictor for response to anti-vascular endothelial growth factor therapy in diabetic macular edema. Am J Ophthalmol. 2015;159(85–91):e81–3.
13. Sonoda S, Sakamoto T, Otsuka H, Yoshinaga N, Yamashita T, Kii Y, et al. Responsiveness of eyes with polypoidal choroidal vasculopathy with choroidal hyperpermeability to intravitreal ranibizumab. BMC Ophthalmol. 2013;13:43.
14. Sonoda S, Sakamoto T, Yamashita T, Shirasawa M, Uchino E, Terasaki H, et al. Choroidal structure in normal eyes and after photodynamic therapy determined by binarization of optical coherence tomographic images. Invest Ophthalmol Vis Sci. 2014;55:3893–9.
15. Sonoda S, Sakamoto T, Yamashita T, Uchino E, Kawano H, Yoshihara N, et al. Luminal and stromal areas of choroid determined by binarization method of optical coherence tomographic images. Am J Ophthalmol. 2015;159(1123–31):e1121.
16. Sonoda S, Sakamoto T, Kakiuchi N, Shiihara H, Sakoguchi T, Tomita M, et al. Semi-automated software to measure luminal and stromal areas of choroid in optical coherence tomographic images. Jpn J Ophthalmol. 2017 (in press).
17. Kinoshita T, Mitamura Y, Mori T, Akaiwa K, Semba K, Egawa M, et al. Changes in choroidal structures in eyes with chronic central serous chorioretinopathy after half-dose photodynamic therapy. PLoS One. 2016;11:e0163104.
18. Sonoda S, Sakamoto T, Kuroiwa N, Arimura N, Kawano H, Yoshihara N, et al. Structural changes of inner and outer choroid in central serous chorioretinopathy determined by optical coherence tomography. PLoS One. 2016;11:e0157190.
19. Shirasawa M, Sakamoto T, Terasaki H, Yamashita T, Uchino E, Sonoda S. Objective determination of optimal number of spectral-domain optical coherence tomographic images of retina to average. PLoS One. 2014;9:e110550.
20. Yamashita T, Yamashita T, Shirasawa M, Arimura N, Terasaki H, Sakamoto T. Repeatability and reproducibility of subfoveal choroidal thickness in normal eyes of Japanese using different SD-OCT devices. Invest Ophthalmol Vis Sci. 2012;53:1102–7.
21. Nickla DL, Wallman J. The multifunctional choroid. Prog Retin Eye Res. 2010;29:144–68.
22. Adhi M, Ferrara D, Mullins RF, Baumal CR, Mohler KJ, Kraus MF, et al. Characterization of choroidal layers in normal aging eyes using enface swept-source optical coherence tomography. PLoS One. 2015;10:e0133080.
23. Almeida DR, Zhang L, Chin EK, Mullins RF, Kucukevcilioglu M, Critser DB, et al. Comparison of retinal and choriocapillaris thicknesses following sitting to supine transition in healthy individuals and patients with age-related macular degeneration. JAMA Ophthalmol. 2015;133:297–303.
24. Fleckenstein M, Charbel Issa P, Helb HM, Schmitz-Valckenberg S, Finger RP, Scholl HP, et al. High-resolution spectral domain-OCT imaging in geographic atrophy associated with age-related macular degeneration. Invest Ophthalmol Vis Sci. 2008;49:4137–44.
25. Hassenstein A, Meyer CH. Clinical use and research applications of Heidelberg retinal angiography and spectral-domain optical coherence tomography - a review. Clin Exp Ophthalmol. 2009;37:130–43.